Toward the Development of the Potential with Angular Distortion for Halogen Bond: A Comparison of Potential Energy Surfaces between Halogen Bond and Hydrogen Bond

ARTICLE *in* THE JOURNAL OF PHYSICAL CHEMISTRY A · MAY 2014

Impact Factor: 2.69 · DOI: 10.1021/jp502739c · Source: PubMed

THE JOURNAL OF PHYSICAL CHEMISTRY A

Article

pubs.acs.org/JPCA

Toward the Development of the Potential with Angular Distortion for Halogen Bond: A Comparison of Potential Energy Surfaces between Halogen Bond and Hydrogen Bond

Lili Wang,[†,‡,§] Jun Gao,*[,†] Fuzhen Bi,[†] Bo Song,[∥] and Chengbu Liu[†]

[†]School of Chemistry & Chemical Engineering, [‡]Advanced Research Center for Optics, [§]School of Materials Science and Engineering, Shandong University, Jinan, Shandong 250100, P. R. China

[∥]Shanghai Institute of Applied Physics, Chinese Academy of Sciences, Laboratory of Physical Biology, Shanghai, 201800, P. R. China

ABSTRACT: As noncovalent intermolecular interactions, hydrogen bond (HB) and halogen bond (XB) are attracting increasing attention. In this work, the potential energy surfaces (PESs) of hydrogen and halogen bonds are compared. Twelve halogen-bonded and three hydrogen-bonded models are scanned for analysis using the MP2 level of theory. This work indicates that potential energy surfaces of both HB and XB have angular distortion. The potential well of XB is narrower than that of HB. With the elongation of the bond length, the potential energy surfaces get flatter. The best fitting functions for angular distortion and the flattening character of angular terms are also combined into a modified Buckingham potential. The testing results show that the essential features of the PES, including angular distortion and flattening character, have been reproduced. These results provide a better understanding of halogen and hydrogen bonds and the optimization of halogen bond force fields.

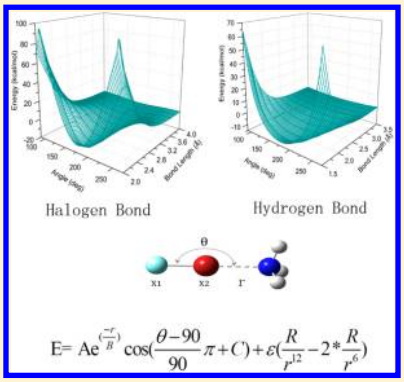

1. INTRODUCTION

Noncovalent intermolecular interactions such as hydrogen bond (HB) and halogen bond (XB) have attracted increasing attention in the past decades.[1−4] HB is a bond interaction that occurs between a hydrogen atom from a molecule or a molecular fragment X−H in which X is more electronegative than H and an atom or a group of atoms in the same or different molecule.[5] XB occurs between an electrophilic region associated with a halogen atom in a molecular entity and a nucleophilic region in another, or the same, molecular entity when there is evidence of a net attractive interaction.[6] XB is analogous to HB;[7] both of them are formed by an electron donor and an electron acceptor, and they have pronounced directionalities.[8] There is an essential difference between HB and XB, i.e., the X halogen atom in XB is bifunctional: simultaneously electronegative and electropositive.[9−11] The electron acceptor in XB is an electronegative halogen atom, while that in HB is a positively charged hydrogen atom. Politzer and Clark[12,13] advance the definition of "σ-hole" to describe the bifunctional property, i.e., σ-hole of the halogen atom interacts with the nucleophile along the covalent bond extension, while the negative region of the electrostatic potential interacts with the electrophile perpendicularly. This property makes XB different from HB. XB interaction was discovered 150 years ago when Frederick Guthrie gave the first report on the halogen-bonded complex formed between iodine and ammonia.[14] However, the importance of the halogen bond has been observed in recent years.[7] It is clear that XB becomes more and more attractive in fields such as crystal engineering,[15] functional materials,[16−20] molecular recognition,[1,21,22] biomolecular systems,[23−25] drug discovery,[26,27] and supramolecular chemistry.[28]

HB and XB are both noncovalent interactions. Many experimental and theoretical works have been conducted to understand these interactions. For example, quantum mechanical (QM),[29] molecular mechanical (MM),[30−32] and QM/MM methods are applied to the theoretical study of the properties of halogen bond systems.[33,34] These works indicate that the interactions of electrostatic effect, polarization, dispersion contribution, and charge transfer are all important for the formation process of halogen and hydrogen bonds. Nevertheless, generating intermolecular potentials with sufficient accuracy is still a challenging subject[35] which needs high-level quantum chemical methods.[36]

The force field (FF) of the hydrogen bond is well-studied, whereas the FF of the halogen bond is still under study;[37,38] this noncovalent interaction cannot be described by conventional FF for the anisotropic distribution of the charge density on the halogen atoms.[39] In 2011, Ibrahim developed the first force field for halogen bond where the positive region centering on the halogen atom was represented by an extra point of charge (EP).[30,31] The Jorgensen group modified OPLS-AA force field to treat halogen bond and tested an application to potent anti-HIV agents.[32] Carter et al. derived a set of simple

Special Issue: International Conference on Theoretical and High Performance Computational Chemistry Symposium

Received: March 19, 2014
Revised: May 26, 2014
Published: May 29, 2014

   dx.doi.org/10.1021/jp502739c | J. Phys. Chem. A 2014, 118, 9140−9147

directional potential energy functions to model the shape and electrostatic properties of halogens, which constituted a set of potential energy functions for a force field for biological halogen bonds (ff BXB).[40] Our group also developed a polarizable ellipsoidal force field (PEff) for halogen bond, in which the anisotropic charge distribution was represented with the combination of a negative charged sphere and a positively charged ellipsoid.[41] Recently, a polarizable multipole force field has been applied to organochlorine compounds.[42]

For bonded interactions, bond stretching, bond angle and dihedral angle terms are commonly adopted in AMBER and CHARMM force fields.[43−45] The harmonic potential is a good approximation for these terms and can get sufficient accuracy results around equivalent regions. For noncovalent interactions where the coulomb interaction and van de Walls interaction terms are used, the depth of the potential wells is relative small and reproducing the whole potential energy surface accurately is important for free-energy calculation. Hence, a systematic comparison of the potential energy surface between HB and XB is beneficial for the design and improvement of current force fields.

In this work, a comparison of the potential energy surfaces was made between hydrogen bond and halogen bond. Twelve XB and three HB models were scanned for analysis using the MP2 level of theory. The potential energy surfaces were then divided into bond length and bond angle portions. Some functions, such as cosine and power functions, were used to fit bond length and bond angle curve. Then, the fitting functions were combined into a Buckingham potential[55,56] to reproduce the character of the potential energy surface.

2. MATERIALS AND METHODS

Twelve halogen-bonded and three hydrogen-bonded models were selected in this work. All these models were then adopted to scan the potential energy surfaces. To simplify the calculation, the symmetries of the models were considered and the effect of hydrogen atom of NH_3 on the potential energy surface was considered to be relatively small. So, as shown in Figure 1, two variables remained: the bond angle θ and the bond length R. For all models, the bond angles were scanned from 90° to 270° by a step of 2°. The ranges of scanned bond length were different for HB and XB models. The halogen bond lengths were scanned from 1.6 to 5 Å, and the HB lengths were scanned from 0.5 to 4.9 Å; a step of 0.2 Å was used for both of them. The total scanned points for all 15 models were 25 935 in this work.

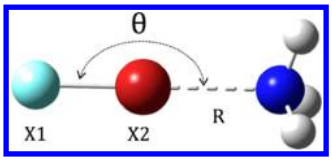

Figure 1. Dynamic scan scheme for the 15 calculation models (12 XB models and 3 HB models). X2 is the donor atom of XB or HB, which is a halogen atom in XB models and hydrogen atom in HB models. X1 is the halogen atom bonding to X2 in the X1−X2 molecule, which affects the various physical behaviors of X2. θ is the XB or HB bond angle. R is the bond length for XB or HB.

All calculations were performed in the second-order Møller−Plesset perturbation level of theory (MP2) using the Gaussian 09 program.[46] This level of theory was adequate for providing reasonably results for weakly bonded interactions.[47−49] The aug-cc-pVTZ basis set was used for the geometry optimization of monomers and dimers (aug-cc-pVTZ-pp for bromine and iodine). The convergence criterion of SCF was 10^{-6}. To calculate the bonding energies of dimer molecular systems, the basis set superposition error (BSSE) was considered.[50] According to BSSE, the calculated interaction energies became too high. Hence, the bond energies of XB and HB here were calculated with BSSE correction. The bond energies of dimers were calculated by the formula $E(\text{interaction}) = E(\text{AB}) - E(\text{A}) - E(\text{B}) + E(\text{BSSE})$. To discern the relative contribution of the interaction energy components, the energy decomposition analysis was calculated by the density functional theory combined with the symmetry adapted perturbation theory (DFT-SAPT) using MOLPRO 2010.1 programs.[51] This method promised to yield results that were in good agreement with those calculated by SAPT method but with a much smaller computational cost.[52]

The potential energy surfaces were fitted by different functions. After systematic tests, we selected a cosine function and power function to fit the angular part of XB and HB, respectively. The bond length term was fitted by an exponential function for both XB and HB. As shown in eq 1, E is the relative energy, θ bond angle, A half peak height of the potential well, and E_0 a constant. E_0 and A were fitting parameters.

$$E = E_0 + A\cos\left(\frac{\theta - 90}{90}\pi\right) \quad (1)$$

Equation 1 provided sufficiently good fitting results for XB models, but the fitting results for HB models were relative bad. Our tests indicated that the power function shown in eq 2 provided relatively accurate fitting. In eq 2, both m and p were fitting parameters.

$$E = m|\theta - 180|^p \quad (2)$$

To describe the decay character of the angular distortion with the elongation of bond length, an exponential function eq 3 was selected. In eq 3, R value was bond length and K and B were fitting parameters.

$$E = Ke^{(-R/B)} \quad (3)$$

3. RESULTS AND DISCUSSIONS

3.1. Comparison of the Potential Surfaces between the XB and HB Models. After screening and comparing all XB and HB models, we summarize similarities and differences of potential energy surfaces of these two models. Figure 2 shows the potential energy surfaces of XB and HB representative models. The left panel is the potential energy surface for model F−Br···NH_3, and the right panel is the potential energy surface for model F−H···NH_3. To compare the potential energy surfaces between these two models clearly, the range of the bond length for XB model and HB model is chosen to be 2−4 Å and 1.5−3.5 Å, respectively, in Figure 2. First, the potential energy surfaces of both HB and XB have angular distortion; it makes sense that both HB and XB are directional.[53,54] Second, the potential well of XB is narrower than that of HB, which indicates that XB is more directional than HB. Third, with the elongation of bond length, the potential energy surfaces get flatter, which indicates that the angular distortion of XB and HB becomes weaker with the elongation of bond length. It also means that the potential

dx.doi.org/10.1021/jp502739c | J. Phys. Chem. A 2014, 118, 9140−9147

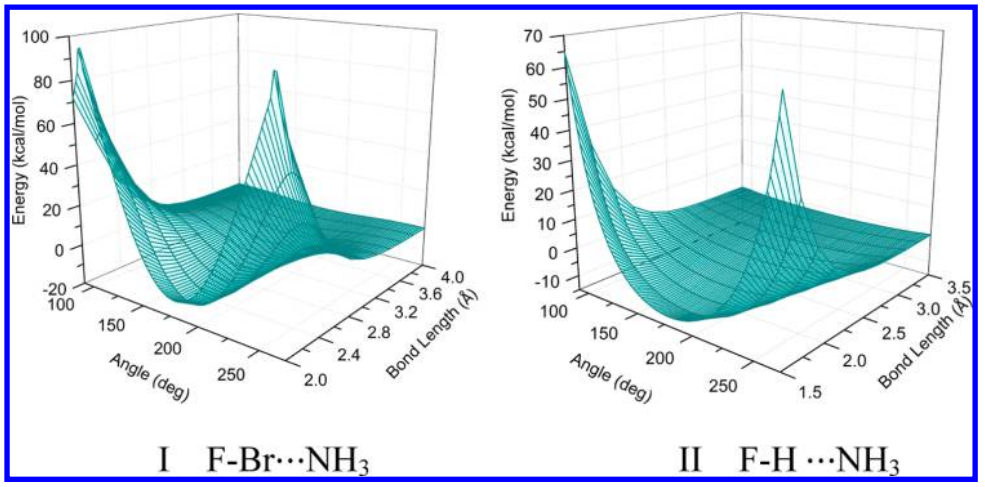

Figure 2. Comparison of the potential energy surfaces of the halogen bond and hydrogen bond. Panel I is the potential surface map for XB model F−Br···NH_3; panel II is the potential surface map for HB model F−H···NH_3.

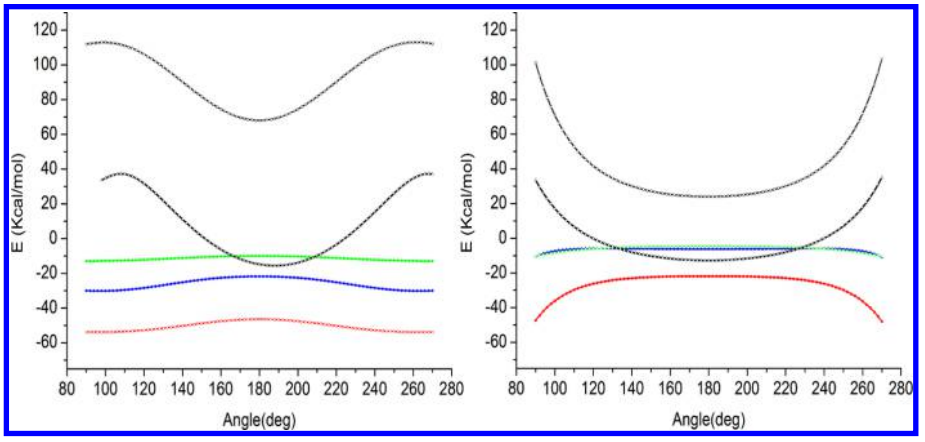

Figure 3. Variation of energy components with halogen (hydrogen) bond angle. The left panel is F−Br···NH_3 and the right panel is F−H···NH_3. The components are exchange−repulsion (black), electrostatic (red), dispersion (green dashed), and induction (blue dash-dot); the heavy black line represents the total.

energy surfaces of HB and XB are similar in the long bond length region.

It is interesting that HB and XB are both directional, but their potential energy surfaces in short bond length region are not similar as expected. To get a better understanding, the SAPT(DFT) analysis method was adopted to analyze the energy components of the potential energy surfaces at equivalent bond length. As shown in Figure 3, the energy components of SAPT(DFT) decomposition with halogen (hydrogen) bond angle at the equilibrium bond lengths were plotted. The left panel is F−Br···NH_3 and the right panel is F−H···NH_3. We used θ (see Figure 1) to denote the bond angle. It is clear that the binding energy is dominated by the electrostatic term for both hydrogen bond and halogen bond, although there are substantial contributions from induction and dispersion. However, none of these terms vary much with θ, and such variation of the electrostatic energy does not favor the linear geometry. It is well-established that the structures of hydrogen-bonded complexes are attributed to electrostatic interactions alone, and those structures can be predicted very successfully using a model comprising accurate distributed multipolar electrostatics and a simple hard-sphere repulsion.[55−57] At the same time, the strong analogies in structures between corresponding halogen-bonded and hydrogen-bonded complexes lead to a general assumption that the structures of the halogen-bonded complexes are attributed to electrostatics alone. Our results indicate that the linearity of the hydrogen bond or halogen bond is due to an exchange−repulsion term rather than electrostatic term.[58] Furthermore, the fitting function of the angular term should also work on the exchange−repulsion term for the similarity of their curves, as discussed in the next section.

3.2. Fitting the Angular Term of Potential Energy Surfaces. As discussed in last section, the potential energy surfaces of both HB and XB show angular distortion. The distortion varied with substitution groups (atoms) of halogen atoms. We selected compounds comprising covalent halogen atom Br as an example. As shown on the upper panel of Figure 4, the relative energies versus the halogen bond angle at the equilibrium bond lengths were plotted. It was evident that the potential energy wells of the models were gradually getting narrower as the terminal halogen atom changed from F to I. Furthermore, the bonding energies were getting weaker from F to I. This indicated that strong halogen bonds had stronger angular distortion than weak halogen bonds. Such properties were also discussed in other works.[41,53] The changes in hydrogen-bonded models were not as significant as those in halogen-bonded models. But the potential well of the F−H···

dx.doi.org/10.1021/jp502739c | J. Phys. Chem. A 2014, 118, 9140−9147

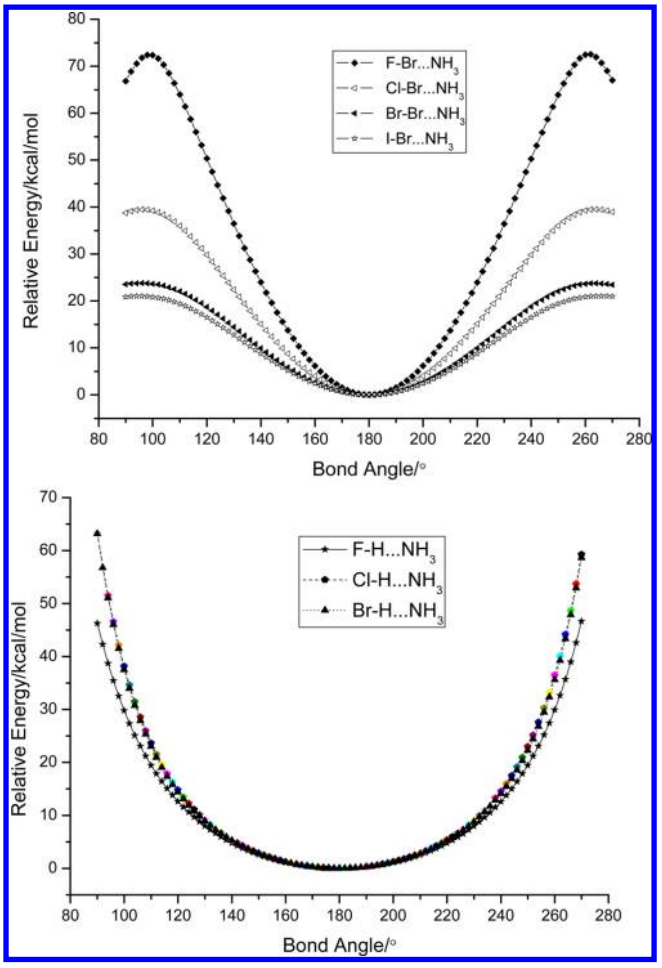

Figure 4. Distortion of interaction energy with halogen (hydrogen) bond angle at equilibrium bond lengths. The upper panel is the plot for the XB models and the lower is the plot for the HB models.

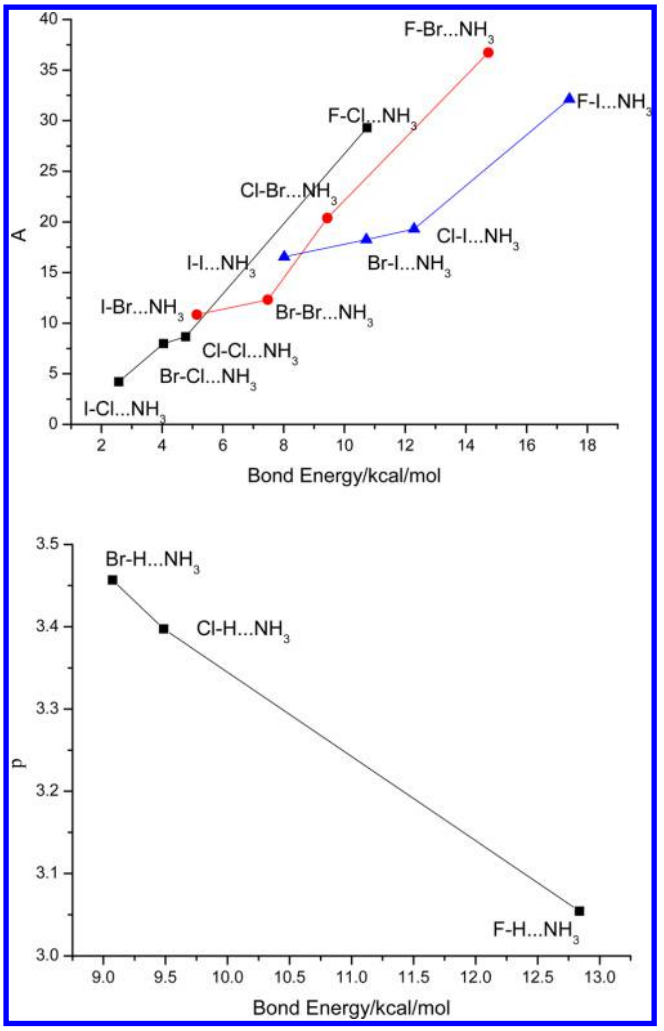

Figure 5. Plots of bond energy versus the *A* value for the XB models (upper panel) and the *p* value for the HB models (lower panel).

Table 1. Bond Energies and Fitting Parameters of the X2 (or H)···NH_3 Interactions in the X1−X2 (or H)···NH_3 Models

model	bond energy (kcal/mol)	*A* value for XB; *p* value for HB	R^2
F−Br···NH_3	14.74	36.73	0.9898
Cl−Br···NH_3	9.44	20.38	0.9981
Br−Br···NH_3	7.48	12.30	0.9987
I−Br···NH_3	5.14	10.84	0.9991
F−Cl···NH_3	10.74	29.31	0.9959
Cl−Cl···NH_3	4.78	8.65	0.9926
Br−Cl···NH_3	4.04	7.99	0.9934
I−Cl···NH_3	2.57	4.21	0.9852
F−I···NH_3	17.41	32.14	0.9901
Cl−I···NH_3	12.30	19.32	0.9972
Br−I···NH_3	10.72	18.25	0.9975
I−I···NH_3	8.02	16.55	0.9980
F−H···NH_3	12.19	3.05	0.9955
Cl−H···NH_3	8.74	3.40	0.9930
Br−H···NH_3	7.71	3.46	0.9918

NH_3 was slightly wider than that of other hydrogen-bonded models. It made sense that angular distortion was driven by the nonspherical character of bonded halogen (hydrogen) atom, which was oblate in shape, with a radius in the direction away from the bond smaller than that perpendicular to the bond.[58] For dimers with the same bonded halogen (hydrogen) atom, the substitution groups (atoms) that formed a stronger covalent bond developed a more nonspherical character of halogen (hydrogen) atoms. Nevertheless, the electron density of the hydrogen atom was relatively small and resulted in no sensitive

Table 2. Fitted Parameters *K*, *B*, and R^2 for the Flattening of the Potential Energy Surfaces with the Elongation of the Bond Length

model	*K*	*B*	R^2
F−Br···NH_3	2259	0.55	0.9819
Cl−Br···NH_3	2476	0.55	0.9764
Br−Br···NH_3	2343	0.55	0.9722
I−Br···NH_3	2698	0.54	0.9729
F−Cl···NH_3	2003	0.50	0.9669
Cl−Cl···NH_3	3401	0.50	0.9677
Br−Cl···NH_3	955	0.50	0.9653
I−Cl···NH_3	3330	0.50	0.9612
F−I···NH_3	6285	0.45	0.9886
Cl−I···NH_3	5798	0.46	0.9899
Br−I···NH_3	5707	0.46	0.9894
I−I···NH_3	6036	0.46	0.9906
F−H···NH_3	4911	0.33	0.9974
Cl−H···NH_3	4058	0.36	0.9919
Br−H···NH_3	4267	0.34	0.9891

dx.doi.org/10.1021/jp502739c | J. Phys. Chem. A 2014, 118, 9140−9147

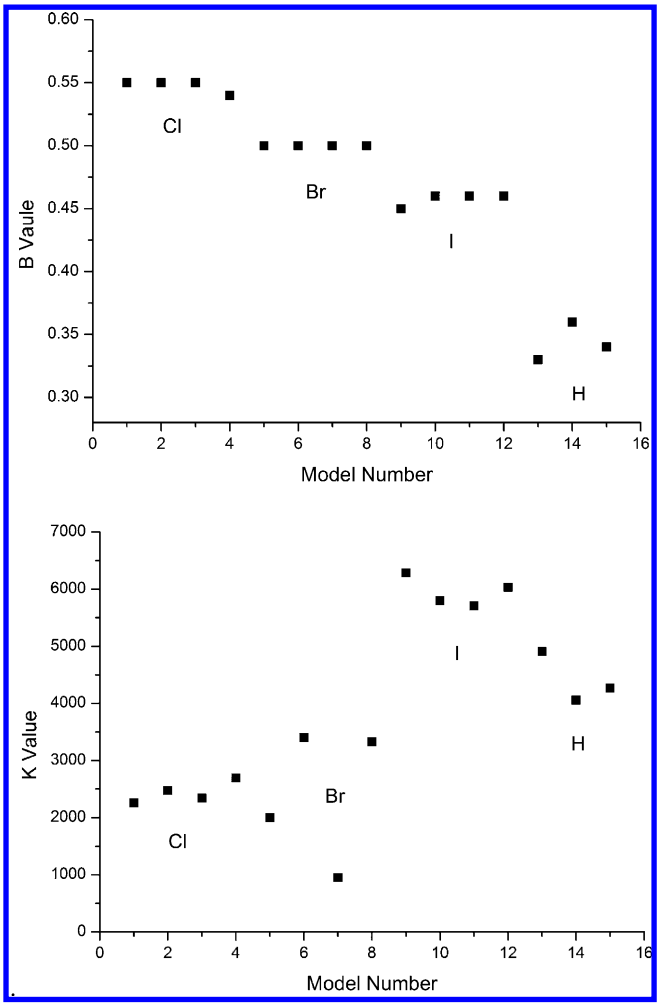

Figure 6. Distribution of K and B values for all halogen-bonded and hydrogen-bonded models.

Table 3. Parameters of Eq 4 for Tested Models F−X···NH_3 (X = Cl, Br, and I)

model	R	A	B	C	ε
F−Cl···NH_3	2.23	1900	0.40	0.60	3.0
F−Br···NH_3	2.29	2500	0.50	0.62	5.55
F−I···NH_3	2.44	4000	0.40	0.18	5.34

response to the substitution atom. At the same time, the bond energy of F−H···NH_3 was relatively higher than that of the other two models (see the lower panel of Figure 4). It seemed that a strong hydrogen bond might get a weaker angular distortion. Our data set was too small to draw a conclusion; further evaluations are needed.

To describe the angular distortion of the models, we tested various functions to fit the relative energy curves at equilibrium bond lengths. The tests indicated that eq 1 worked well for halogen-bonded models and eq 2 functioned well for hydrogen-bonded models. Furthermore, we also tested the fitting function for exchange−repulsion term of SAPT(DFT) energy decomposition, and the same result was acheieved as their curves were similar to that of the angular term. The fitting parameters for A values of XB models, p values of HB models, and R^2 values are listed in Table 1. The R^2 values of all models fell in a range of 0.98−1, which indicated that the selected fitting functions were acceptable for all models. The range of A values was distributed from 4 to 37, and that of the p values was from 3 to 3.5. According to their covalent bonded halogen atoms or hydrogen atom, all the 15 models were divided into four groups: Cl, Br, I, and H. Interestingly, the $A(p)$ values were closely correlated with their bonding energy in each group. As shown in Figure 5, for halogen-bonded models, a compound with a larger A value showed relatively high bond energy; for hydrogen-bonded models, a compound with a larger p value showed relatively low bond energy. It made sense that the A value corresponded to the "half well depth" of the cosine function and the p value corresponded to the decay rate of the power function. Therefore, a relatively larger A value meant higher bond energy and strong angular distortion, and a relatively larger p value meant higher decay rate and strong angular distortion.

3.3. Flattening of the Potential Energy Surfaces with the Elongation of the Bond Length. As shown in section 3.1, the potential energy surfaces get flatter with the elongation of the bond length. To have a better understanding of the decay properties of the energy surfaces, eq 3 was used to fit all models, and the potential energy curves along the bond angle 90° were selected. The fitting parameters of K, B, and R^2 values are listed in Table 2. The R^2 values of all models fell in a range of 0.96−1, which indicated that the selected fitting functions were acceptable for all models. The trends of K values were not very explicit. If covalent halogen atoms of the models were compared, K values were similar in models involving Br and Cl, whereas K values of models involving I were relatively high. All the K values of the hydrogen-bonded models were similar, which distinguished these models from halogen-bonded models (see the lower panel of Figure 6). We noticed that K values of models involving Br and Cl were also similar, which was due to the similar bonding properties of these models; the bonding energies for each pair were relatively close (see Table 1).

Interestingly, the fitted B values were closely related to their covalent halogen (or H) atom type. As shown in Table 2 and Figure 6, B values of models involving Cl, Br, or I and hydrogen-bonded models were around 0.5 and 0.3, respectively. It should be noted that the B values were fitted from the decay curves of potential energy surfaces and the B values indicated the decay rate of an exponential function. Therefore, the dominant contribution to the decay properties came from covalent halogen atom (or H) itself. According to the SAPT analyses, the X-bond strength increased with increasing size of halogen atom, which could be associated with the anisotropy of the halogen atom, being larger in the case of heavier atoms.[59] Also, as the electronegativity of the substituents added to the halogen bond donor increased, the halogen bond length became shorter and the halogen bond strength increased.[52] We noticed that eq 3 was adopted in the Buckingham potential,[55,56] which described the Pauli repulsion energy and van der Waals energy. Thus, taking account of the balance between the attractive terms, such as induction, dispersion, and electrostatics, and the exchange−repulsion term is necessary in describing the binding process of halogen and hydrogen bonds.[58]

The potential applications of fitting functions were to improve the force fields of halogen or hydrogen bonds. Compared with the angular distortion term, the exponential function in eq 3 was used to fit both hydrogen- and halogen-bonded models, and the fitting parameter B depended only on the covalent halogen (or H) atom. Hence, we suggested that eq 3 should be helpful for improving both hydrogen and halogen

dx.doi.org/10.1021/jp502739c | J. Phys. Chem. A 2014, 118, 9140−9147

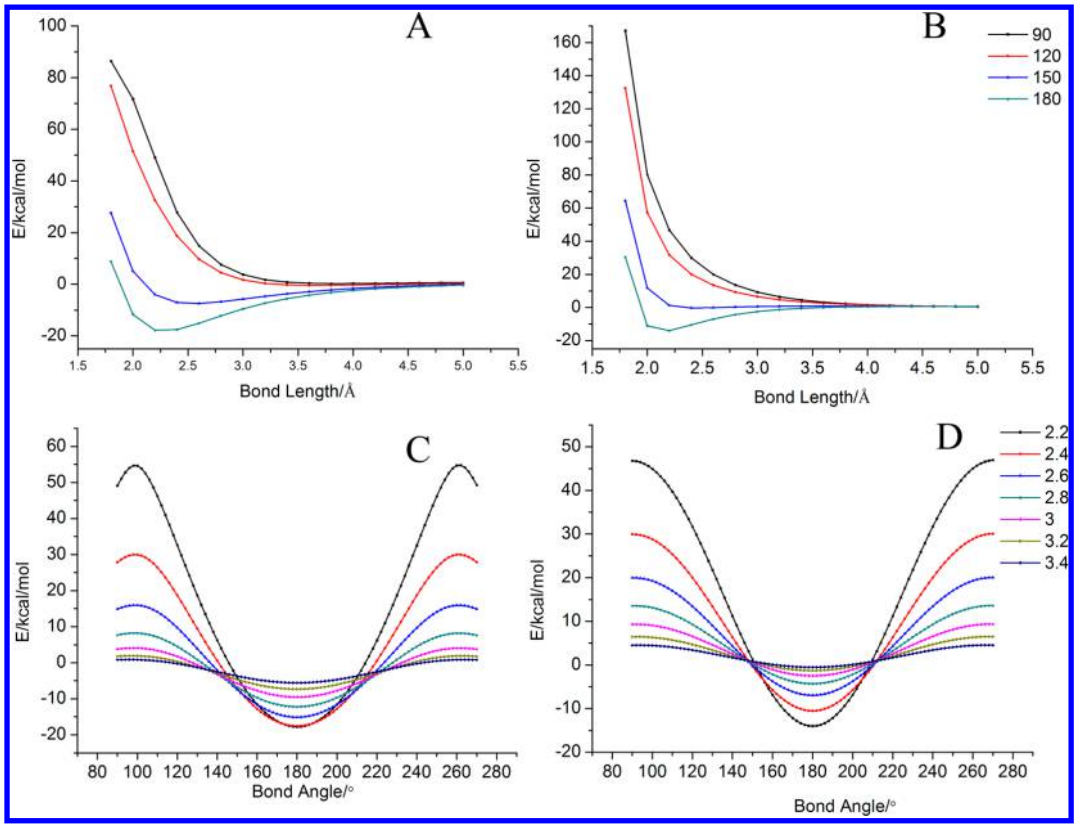

Figure 7. Angular distortion of potential energy curves: (A) ab initio level at different angles (MP2/aug-cc-pVTZ level); (B) fitting results at different angles; (C) ab initio level at different distances (MP2/aug-cc-pVDZ level); (D) fitting results at different distances.

bond force fields. Our study also indicated that eqs 1 and 3 were helpful for improving the current force fields which did not account for the anisotropic distribution of the charge density on the halogen atoms.[30,31]

3.4. Testing Analytical Form of Potential Energy Surfaces for Halogen Bond. There were a limited number of models in our test. The complicity of the force field and molecular modeling were still not covered. However, at least we provided a potential function which had relatively clear physical meaning for choice. In order to test the potential application of the fitting functions, eq 1 and 3 are combined to get a new form of potential energy surfaces of halogen bond (as shown in eq 4).

$$E = Ae^{(-r/B)}\cos\left(\frac{\theta - 90}{90}\pi + C\right) + \varepsilon\left(\frac{R}{r^{12}} - 2\frac{R}{r^{6}}\right) \quad (4)$$

In eq 4, θ is bond angle, r bond length of halogen bond, ε the parameter of Lennard-Jones potential, and R equilibrium bond length. A and C are constants. A and B were taken from our fitted values, and then they were optimized. Therefore, only two parameters, C and ε, were in need for fitting. The first term was a modified Buckingham potential[55,56] in which the attraction term was replaced by the Lennard-Jones potential.[60] On the basis of our fitting results, a cosine function was added to the first term of eq 4.

The parameter values were derived in a stepwise fashion. The GAFF force field was used to describe the testing complexes, whereas the corresponding parameters for the covalent halogen atom were derived by the protocol of our previous work.[41] Partial atomic charges were assigned according to the restrained electrostatic potential (RESP) approach as recommended in the parametrization protocol of the GAFF force field.[61] The noncovalent interaction between halogen atom and N atom of the GAFF force field was replaced by eq 4. The parameters were optimized with the nonlinear least-squares fit procedure.

We selected only F−X···NH_3 (X = Cl, Br, and I) as test cases. The parameters of these models are listed in Table 3. The angular distortion and the flattening of the potential energy surface of binding energy for F−X···NH_3 complex are illustrated in Figure 7A−D. The essential feature of the ab initio PES seemed to be reproduced by our proposed potential function. Additionally, the differences of interaction energy from ab initio values were slightly larger near 90°; this is attributed to the overestimation of noncovalent interactions at the MM level. At the same time, the MP2 and QCISD methods systematically overestimated the halogen-bonding energy, compared with the CCSD(T) method.[62,63] Furthermore, the polarization term was not included in eq 4, and we did not consider fitting the polarization function in our fitting process. As is well-known, the polarization effect played an important role in halogen bond, enhancing the bonding process.[64] A potential function based on Buckingham-like potential which deals with both angular distortion and polarization effects is now under development in our group.

4. CONCLUSION

In this work, the potential energy surfaces were compared between halogen and hydrogen bond models, which indicated that the potential energy surfaces of both HB and XB have angular distortion. The potential well of XB was narrower than that of HB. The energy components of SAPT decomposition showed that the dominant contribution to angular distortion came from exchange−repulsion term. At the same time, with

dx.doi.org/10.1021/jp502739c | J. Phys. Chem. A 2014, 118, 9140−9147

the elongation of the bond length, the potential energy surface gradually got flatter.

To get a better understanding of these potential energy surfaces, the best fitting functions for the angular distortion term and the flattening character of the angular term were studied. The angular distortion of halogen bonds can be described by a cosine function, whereas a power function was much better for hydrogen bonds. An exponential function was also adopted to describe the flattening character of angular distortion with bond elongation; the fitted B value was related to halogen atom or hydrogen atom only. These fitting functions were then combined to describe the anisotropic distribution of the charge density on halogen atoms. The modified Buckingham potential can reproduce the essential feature of the PES including angular distortion and flattening character.

AUTHOR INFORMATION

Corresponding Author

*E-mail: gaojun@sdu.edu.cn. Phone: +86-531-88363967. Fax: +86-531-88564464.

Notes

The authors declare no competing financial interest.

ACKNOWLEDGMENTS

This work is supported by the National Natural Science Foundation of China (91127014 and 21373124), Doctoral Fund of Ministry of Education of China (20110131120010), and China Postdoctoral Science Foundation (2012M521319). It is also supported by the National Supercomputer Center in Jinan and Shandong University High Performance Computing Center.

REFERENCES

(1) Metrangolo, P.; Neukirch, H.; Pilati, T.; Resnati, G. Halogen Bonding Based Recognition Processes: A World Parallel to Hydrogen Bonding. *Acc. Chem. Res.* **2005**, *38*, 386−395.

(2) Bent, H. A. Structural Chemistry of Donor-Acceptor Interactions. *Chem. Rev. (Washington, DC, U. S.)* **1968**, *68*, 587−648.

(3) Beale, T. M.; Chudzinski, M. G.; Sarwar, M. G.; Taylor, M. S. Halogen Bonding in Solution: Thermodynamics and Applications. *Chem. Soc. Rev.* **2013**, *42*, 1667−1680.

(4) Hassel, O. Structural Aspects of Interatomic Charge-Transfer Bonding. *Science* **1970**, *170*, 497−502.

(5) Arunan, E.; Desiraju, G. R.; Klein, R. A.; Sadlej, J.; Scheiner, S.; Alkorta, I.; Clary, D. C.; Crabtree, R. H.; Dannenberg, J. J.; Hobza, P.; et al. Definition of the Hydrogen Bond (IUPAC Recommendations 2011). *Pure Appl. Chem.* **2011**, *83*, 1637−1641.

(6) Desiraju, G. R.; Ho, P. S.; Kloo, L.; Legon, A. C.; Marquard, R.; Metrangolo, P.; Politzer, P.; Resnati, G.; Rissanen, K. Definition of the Halogen Bond (IUPAC Recommendations 2013). *Pure Appl. Chem.* **2013**, *85*, 1711−1713.

(7) Metrangolo, P.; Resnati, G. Chemistry - Halogen versus Hydrogen. *Science* **2008**, *321*, 918−919.

(8) Legon, A. C. The Halogen Bond: An Interim Perspective. *Phys. Chem. Chem. Phys.* **2010**, *12*, 7736−7747.

(9) Bouchmella, K.; Boury, B.; Dutremez, S. G.; van der Lee, A. Molecular Assemblies from Imidazolyl-Containing Haloalkenes and Haloalkynes: Competition between Halogen and Hydrogen Bonding. *Chem.—Eur. J.* **2007**, *13*, 6130−6138.

(10) Aakeröy, C. B.; Fasulo, M.; Schultheiss, N.; Desper, J.; Moore, C. Structural Competition between Hydrogen Bonds and Halogen Bonds. *J. Am. Chem. Soc.* **2007**, *129*, 13772−13773.

(11) Liu, X.; Cheng, J.; Li, Q.; Li, W. Competition of Hydrogen, Halogen, and Pnicogen Bonds in the Complexes of HArF with XH_2P (X = F, Cl, and Br). *Spectrochim. Acta, Part A* **2013**, *101*, 172−177.

(12) Politzer, P.; Murray, J. S. Halogen Bonding and Beyond: Factors Influencing the Nature of CN−R and SiN-R Complexes with F−Cl and Cl_2. *Theor. Chem. Acc.* **2012**, 131.

(13) Meazza, L.; Foster, J. A.; Fucke, K.; Metrangolo, P.; Resnati, G.; Steed, J. W. Halogen-Bonding-Triggered Supramolecular Gel Formation. *Nat. Chem.* **2013**, *5*, 42−47.

(14) Guthrie, F. On the Iodide of Iodammonium. *J. Chem. Soc.* **1863**, *16*, 239−244.

(15) Metrangolo, P.; Resnati, G.; Pilati, T.; Biella, S., Halogen Bonding in Crystal Engineering. In *Halogen Bonding*; Metrangolo, P., Resnati, G., Eds.; Springer: Berlin Heidelberg, 2008; Vol. *126*, pp 105−136.

(16) Metrangolo, P.; Meyer, F.; Pilati, T.; Resnati, G.; Terraneo, G. Halogen Bonding in Supramolecular Chemistry. *Angew. Chem., Int. Ed.* **2008**, *47*, 6114−6127.

(17) Voth, A. R.; Hays, F. A.; Ho, P. S. Directing Macromolecular Conformation through Halogen Bonds. *Proc. Natl. Acad. Sci. U.S.A.* **2007**, *104*, 6188−6193.

(18) Shirman, T.; Kaminker, R.; Freeman, D.; van der Boom, M. E. Halogen-Bonding Mediated Stepwise Assembly of Gold Nanoparticles onto Planar Surfaces. *ACS Nano* **2011**, *5*, 6553−6563.

(19) Fourmigué, M. Halogen Bonding in Conducting or Magnetic Molecular Materials. *Struct. Bonding (Berlin, Ger.)* **2008**, *126*, 181−207.

(20) Bruce, D. W.; Metrangolo, P.; Meyer, F.; Pilati, T.; Praesang, C.; Resnati, G.; Terraneo, G.; Wainwright, S. G.; Whitwood, A. C. Structure-Function Relationships in Liquid-Crystalline Halogen-Bonded Complexes. *Chem.—Eur. J.* **2010**, *16*, 9511−9524.

(21) Cavallo, G.; Metrangolo, P.; Pilati, T.; Resnati, G.; Sansotera, M.; Terraneo, G. Halogen Bonding: A General Route in Anion Recognition and Coordination. *Chem. Soc. Rev.* **2010**, *39*, 3772−3783.

(22) Caballero, A.; Zapata, F.; White, N. G.; Costa, P. J.; Felix, V.; Beer, P. D. A Halogen-Bonding Catenane for Anion Recognition and Sensing. *Angew. Chem., Int. Ed.* **2012**, *51*, 1876−80.

(23) Auffinger, P.; Hays, F. A.; Westhof, E.; Ho, P. S. Halogen Bonds in Biological Molecules. *Proc. Natl. Acad. Sci. U.S.A.* **2004**, *101*, 16789−16794.

(24) Panigrahi, S. K.; Desiraju, G. R. Strong and Weak Hydrogen Bonds in the Protein-Ligand Interface. *Proteins: Struct., Funct., Bioinf.* **2007**, *67*, 128−141.

(25) Voth, A. R.; Khuu, P.; Oishi, K.; Ho, P. S. Halogen Bonds as Orthogonal Molecular Interactions to Hydrogen Bonds. *Nat. Chem.* **2009**, *1*, 74−79.

(26) Hardegger, L. A.; Kuhn, B.; Spinnler, B.; Anselm, L.; Ecabert, R.; Stihle, M.; Gsell, B.; Thoma, R.; Diez, J.; Benz, J.; et al. Halogen Bonding at the Active Sites of Human Cathepsin L and Mek1 Kinase: Efficient Interactions in Different Environments. *ChemMedChem.* **2011**, *6*, 2048−2054.

(27) Bartashevich, E. V.; Tsirelson, V. G. Atomic Dipole Polarization in Charge-Transfer Complexes with Halogen Bonding. *Phys. Chem. Chem. Phys.* **2013**, *15*, 2530−2538.

(28) Metrangolo, P.; Meyer, F.; Pilati, T.; Proserpio, D. M.; Resnati, G. Highly Interpenetrated Supramolecular Networks Supported by N···I Halogen Bonding. *Chem.—Eur. J.* **2007**, *13*, 5765−5772.

(29) Parker, A. J.; Stewart, J.; Donald, K. J.; Parish, C. A. Halogen Bonding in DNA Base Pairs. *J. Am. Chem. Soc.* **2012**, *134*, 5165−5172.

(30) Ibrahim, M. A. A. AMBER Empirical Potential Describes the Geometry and Energy of Noncovalent Halogen Interactions Better than Advanced Semiempirical Quantum Mechanical Method PM6-DH2X. *J. Phys. Chem. B* **2012**, *116*, 3659−3669.

(31) Ibrahim, M. A. A. Molecular Mechanical Study of Halogen Bonding in Drug Discovery. *J. Comput. Chem.* **2011**, *32*, 2564−2574.

(32) Jorgensen, W. L.; Schyman, P. Treatment of Halogen Bonding in the OPLS-AA Force Field: Application to Potent Anti-HIV Agents. *J. Chem. Theory Comput.* **2012**, *8*, 3895−3901.

(33) Lu, Y.; Shi, T.; Wang, Y.; Yang, H.; Yan, X.; Luo, X.; Jiang, H.; Zhu, W. Halogen Bonding: A Novel Interaction for Rational Drug Design? *J. Med. Chem.* **2009**, *52*, 2854−2862.

(34) Ibrahim, M. A. A. Performance Assessment of Semiempirical Molecular Orbital Methods in Describing Halogen Bonding: Quantum

Mechanical and Quantum Mechanical/Molecular Mechanical-Molecular Dynamics Study. *J. Chem. Inf. Model.* **2011**, *51*, 2549−2559.
(35) Stone, A. J. Intermolecular Potentials. *Science* **2008**, *321*, 787−789.
(36) Jurecka, P.; Sponer, J.; Cerny, J.; Hobza, P. Benchmark Database of Accurate (MP2 and CCSD(T) Complete Basis Set Limit) Interaction Energies of Small Model Complexes, DNA Base Pairs, and Amino Acid Pairs. *Phys. Chem. Chem. Phys.* **2006**, *8*, 1985−1993.
(37) Korth, M. Third-Generation Hydrogen-Bonding Corrections for Semiempirical Qm Methods and Force Fields. *J. Chem. Theory Comput.* **2010**, *6*, 3808−3816.
(38) Ibrahim, M. A. A. Molecular Mechanical Study of Halogen Bonding in Drug Discovery. *J. Comput. Chem.* **2011**, *32*, 2564−2574.
(39) Lu, Y.; Shi, T.; Wang, Y.; Yang, H.; Yan, X.; Luo, X.; Jiang, H.; Zhu, W. Halogen Bonding—A Novel Interaction for Rational Drug Design? *J. Med. Chem.* **2009**, *52*, 2854−2862.
(40) Carter, M.; Rappé, A. K.; Ho, P. S. Scalable Anisotropic Shape and Electrostatic Models for Biological Bromine Halogen Bonds. *J. Chem. Theory Comput.* **2012**, *8*, 2461−2473.
(41) Du, L.; Gao, J.; Bi, F.; Wang, L.; Liu, C. A Polarizable Ellipsoidal Force Field for Halogen Bonds. *J. Comput. Chem.* **2013**, *34*, 2032−2040.
(42) Mu, X.; Wang, Q.; Wang, L.-P.; Fried, S. D.; Piquemal, J.-P.; Dalby, K. N.; Ren, P.Modeling Organochlorine Compounds and the σ-Hole Effect Using a Polarizable Multipole Force Field. *J. Phys. Chem. B* **2014**, in press.
(43) Case, D. A.; Cheatham, T. E.; Darden, T.; Gohlke, H.; Luo, R.; Merz, K. M.; Onufriev, A.; Simmerling, C.; Wang, B.; Woods, R. J. The Amber Biomolecular Simulation Programs. *J. Comput. Chem.* **2005**, *26*, 1668−1688.
(44) Salomon-Ferrer, R.; Case, D. A.; Walker, R. C. An Overview of the AMBER Biomolecular Simulation Package. *Wiley Interdiscip. Rev.: Comput. Mol. Sci.* **2013**, *3*, 198−210.
(45) Brooks, B. R.; Brooks, C. L.; Mackerell, A. D.; Nilsson, L.; Petrella, R. J.; Roux, B.; Won, Y.; Archontis, G.; Bartels, C.; Boresch, S.; et al. CHARMM: The Biomolecular Simulation Program. *J. Comput. Chem.* **2009**, *30*, 1545−1614.
(46) Frisch, M. J.; Trucks, G. W.; Schlegel, H. B.; Scuseria, G. E.; Robb, M. A.; Cheeseman, J. R.; Scalmani, G.; Barone, V.; Mennucci, B.; Petersson, G. A., et al. *Gaussian 09*, revision A.1; Gaussian, Inc.: Wallingford, CT, 2009.
(47) Bauzá, A.; Alkorta, I.; Frontera, A.; Elguero, J. On the Reliability of Pure and Hybrid DFT Methods for the Evaluation of Halogen, Chalcogen, and Pnicogen Bonds Involving Anionic and Neutral Electron Donors. *J. Chem. Theory Comput.* **2013**, *9*, 5201−5210.
(48) Alkorta, I.; Blanco, F.; Solimannejad, M.; Elguero, J. Competition of Hydrogen Bonds and Halogen Bonds in Complexes of Hypohalous Acids with Nitrogenated Bases. *J. Phys. Chem. A* **2008**, *112*, 10856−10863.
(49) Kniep, F.; Walter, S. M.; Herdtweck, E.; Huber, S. M. 4,4′-Azobis(Halopyridinium) Derivatives: Strong Multidentate Halogen-Bond Donors with a Redox-Active Core. *Chem.—Eur. J.* **2012**, *18*, 1306−1310.
(50) Paizs, B.; Suhai, S. Comparative Study of BSSE Correction Methods at DFT and MP2 Levels of Theory. *J. Comput. Chem.* **1998**, *19*, 575−584.
(51) Werner, H. J.; Knowles, P. J.; Knizia, G.; Manby, F. R.; Schütz, M.; et al. *MOLPRO*, version 2010.1.
(52) Riley, K. E.; Hobza, P. Investigations into the Nature of Halogen Bonding Including Symmetry Adapted Perturbation Theory Analyses. *J. Chem. Theory Comput.* **2008**, *4*, 232−242.
(53) Adhikari, U.; Scheiner, S. Sensitivity of Pnicogen, Chalcogen, Halogen and H-Bonds to Angular Distortions. *Chem. Phys. Lett.* **2012**, *532*, 31−35.
(54) Scheiner, S. Detailed Comparison of the Pnicogen Bond with Chalcogen, Halogen, and Hydrogen Bonds. *Int. J. Quantum Chem.* **2013**, *113*, 1609−1620.
(55) Buckingham, A. D.; Fowler, P. W. Do Electrostatic Interactions Predict Structures of Van Der Waals Molecules? *J. Chem. Phys.* **1983**, *79*, 6426−6428.
(56) Buckingham, A. D.; Fowler, P. W. A Model for the Geometries of Van Der Waals Complexes. *Can. J. Chem.* **1985**, *63*, 2018−2025.
(57) Buckingham, A. D.; Fowler, P. W.; Stone, A. J. Electrostatic Predictions of Shapes and Properties of Van Der Waals Molecules. *Int. Rev. Phys. Chem.* **1986**, *5*, 107−114.
(58) Stone, A. J. Are Halogen Bonded Structures Electrostatically Driven? *J. Am. Chem. Soc.* **2013**, *135*, 7005−7009.
(59) Manna, D.; Mugesh, G. Regioselective Deiodination of Thyroxine by Iodothyronine Deiodinase Mimics: An Unusual Mechanistic Pathway Involving Cooperative Chalcogen and Halogen Bonding. *J. Am. Chem. Soc.* **2012**, *134*, 4269−4279.
(60) Jones, J. E. On the Determination of Molecular Fields. II. From the Equation of State of a Gas. *Proc. R. Soc. London, A* **1924**, *106*, 463−477.
(61) Wang, J.; Wolf, R. M.; Caldwell, J. W.; Kollman, P. A.; Case, D. A. Development and Testing of a General Amber Force Field. *J. Comput. Chem.* **2004**, *25*, 1157−1174.
(62) Lu, Y.-X.; Zou, J.-W.; Wang, Y.-H.; Jiang, Y.-J.; Yu, Q.-S. Ab Initio Investigation of the Complexes between Bromobenzene and Several Electron Donors: Some Insights into the Magnitude and Nature of Halogen Bonding Interactions. *J. Phys. Chem. A* **2007**, *111*, 10781−10788.
(63) Li, R.-Y.; Li, Z.-R.; Wu, D.; Li, Y.; Chen, W.; Sun, C.-C. Study of π Halogen Bonds in Complexes $C_2H_{4-n}F_n$−ClF (n = 0−2). *J. Phys. Chem. A* **2005**, *109*, 2608−2613.
(64) Bi, F.; Gao, J.; Wang, L.; Du, L.; Song, B.; Liu, C. Polarization-Enhanced Bonding Process of Halogen Bond, a Theoretical Study on F−H/F−X (X=F, Cl, Br, I) and Ammonia. *Chem. Phys.* **2013**, *426*, 16−22.